

# Microwave Emission Characteristics of Oil Slicks

A. T. Edgerton,\* D. Meeks,† and D. Williams‡  
Aerojet-General Corporation, El Monte, Calif.

Dependence of microwave emission on oil type, age, film thickness, observational wavelength, antenna viewing angle and polarization was examined in the laboratory. Airborne measurements of controlled oil spills were subsequently performed at wavelengths of 8.1 and 3.2 mm for several refined and crude oil slicks, over a broad range of ocean surface and weather conditions. Oil slicks on the ocean surface provide unique and readily measurable signatures. Lowest amplitude passive microwave signals were of the order of 5°K. A 3°K microwave temperature difference is well within the detection capabilities of airborne passive microwave imaging systems.

## Introduction

A RESEARCH program has been performed by Aerojet-General Corp. to determine the feasibility of using microwave radiometry for detection, identification and surveillance of oil pollution. The study, sponsored by the U.S. Coast Guard, was stimulated by the need for an airborne surveillance system which can detect oil pollution during day and night and in inclement weather. The study encompasses three areas of investigation: 1) theoretical studies, 2) laboratory measurements, and 3) airborne measurements of controlled oil spills. Theoretical studies were concerned with parameters that influence microwave emission from both unpolluted and oil-covered seas. During the laboratory phase, oil films on water were examined as a function of oil-film thickness, physical temperature of the oil-water surfaces, pollutant type, sensor wavelength, antenna polarization, and angle of observation. The airborne measurements consisted of at-sea tests of controlled oil spills off the Southern California coast. Four sets of oil spills, or missions, were performed to obtain data over a variety of sea-surface conditions. The spills, ranging in volume from 220 to 660 gallons, were conducted in the vicinity of long. 119° 08' W and lat. 33° 45' N. Pollutants used for the tests consisted of both refined and crude petroleum and included No. 2 diesel fuel (34.1 API gravity), 26.1 and 21.6 API gravity crude oils, and No. 6175 fuel oil (9.7 API gravity). Microwave measurements were conducted with dual-polarized 3.2- and 8.1-mm sensors. Operational requirements for oil-pollution surveillance were also examined. The study shows that oil slicks on the ocean surface provide unique and readily measurable microwave signatures and that passive microwave images can provide oil-slick detection capabilities over a wide range of sea state and weather conditions. Results of this study are reported in greater detail in Microwave Div. Rept. 1335-2.

## Theoretical Considerations

The microwave region of the electromagnetic spectrum includes wavelengths ranging from near 30 cm to somewhat less than 1 mm (frequencies of about 1-300 GHz). The emission, transmission, scattering, and absorption of microwave radiation are governed by the same physical laws as radiation in the visible and infrared spectral bands. Natural microwave radiation emitted and reflected

from the Earth's surface is generally expressed as the brightness temperature,  $T_b$ , of the surface. Instruments used to measure this radiation are microwave radiometers and they are calibrated with reference to a radiation source of known brightness temperature.

The brightness temperature observed by a radiometer at some height  $h$  above the surface is affected by the atmosphere in several ways, as shown in Fig. 1. First the radiation leaving the surface includes a component,  $\epsilon(\theta)T$ , which is emitted by the surface and a component,  $r(\theta)T_s$ , which consists of reflected incoming radiation,  $T_s$ , emitted by the atmosphere above the surface (plus a component due to the cosmic background). Secondly, on leaving the surface, the radiation is attenuated by the atmosphere in propagating to the radiometer, as indicated by the term  $\tau(h)$  in Eq. (1). Finally, the atmosphere between the radiometer and the surface emits radiation which contributes to the received signal as indicated by the last term of Eq. (1). The brightness temperature measured from a platform at height  $h$  can then be expressed as

$$T_b(\theta, h) = [\epsilon(\theta)T + r(\theta)T_s]\tau(h) + \int_0^h T_A(h) \frac{\partial \tau}{\partial h} dh \quad (1)$$

where  $T$  is the ambient temperature of the surface material,  $T_s$  is the brightness temperature of the sky,  $T_A$  is the ambient temperature of the atmosphere,  $\epsilon$  is the emissivity of the material,  $r$  is the reflectivity of the material ( $r = 1 - \epsilon$ ),  $\tau$  is the transmissivity of the atmosphere, and  $\theta$  is the viewing angle of the antenna.<sup>1</sup>

Water has an emissivity of only about 0.4 and therefore, always appears quite cold. For oil, on the other hand, the emissivity is near 1.0 so that its brightness temperature approaches the actual oil temperature. Water clouds vary in transmissivity virtually from 0.0 to 1.0 depending on thickness and liquid water content (ice cloud transmittance approaches 1.0).

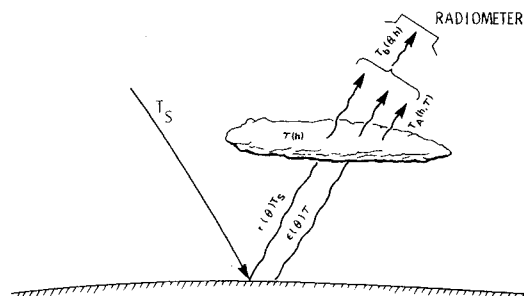


Fig. 1 Sources of measured microwave radiation from airborne or spacecraft platforms.

Presented as Paper 71-1071 at the Joint Conference on Sensing of Environmental Pollutants, Palo Alto, California, November 8-10, 1971; received July 25, 1972.

Index categories: Physical and Biological Oceanography; Sea Pollution Containment and Control.

\*Manager, Earth Resource Programs, Microwave Division.

†Research Oceanographer, Microwave Division.

‡Supervisor, Geosciences Group, Microwave Division; presently self-employed.

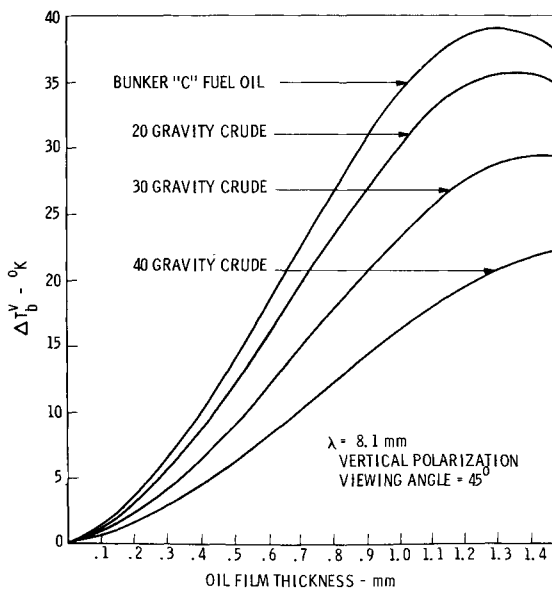


Fig. 2 Vertical brightness temperature increase,  $\Delta T_b^v$ , vs oil film thickness at 8.1-mm wavelength for smooth water surfaces.

Considering that radiation emitted by many natural materials is polarized, Eq. (1) can be written for both horizontal 2) and vertical 3) components. Horizontal and vertical polarizations are defined such that the electrical vectors lie in planes parallel and perpendicular to the Earth's surface, respectively.

$$T_{b,H}(\theta, h) = [\epsilon_H(\theta)T + r_H(\theta)T_s]\tau(h) + \int_0^h T_A \frac{\partial \tau}{\partial h} dh \quad (2)$$

$$T_{b,V}(\theta, h) = [\epsilon_V(\theta)T + r_V(\theta)T_s]\tau(h) + \int_0^h T_A \frac{\partial \tau}{\partial h} dh \quad (3)$$

Subscripts *H* and *V* denote horizontal and vertical polarization, respectively. Only  $\epsilon$  and  $r$  depend on polarization in Eqs. (2) and (3). Thus, polarization strictly relates to characteristics of the surface materials.

The difference between  $T_{b,V}$  and  $T_{b,H}$  for smooth surfaces varies strongly with nadir angle,  $\theta$ , due to the strong angular dependence of  $\epsilon_V(\theta)$  and  $\epsilon_H(\theta)$ . For the most common natural condition of  $T_s \ll T$ , the difference  $T_{b,V} - T_{b,H}$  is always positive and is largest at the Brewster angle (i.e., at that  $\theta$  for which  $\epsilon_V(\theta)$  is a maximum) which, for most natural surfaces occurs near  $\theta = 70^\circ$ . As the surface becomes rougher,  $\epsilon_V(\theta)$  and  $\epsilon_H(\theta)$  approach one another and  $T_{b,V} - T_{b,H}$  decreases.

It is known from theory as well as from experimental observations that for an uncontaminated sea, surface roughness increases the brightness temperature over that obtained for a smooth sea.<sup>2</sup> This is due to the fact that the emissivity of a rough surface is greater than that of a smooth surface of the same material at the same temperature. Oil slicks on the ocean surface affect the radiometric response in at least two important ways. First, the smoothing or damping effect of the oil reduces the sea surface roughness and emissivity which results in a lower radiometric temperature. Second, the emissivity of oil is much greater than that of sea water. Oil films on flat or calm water surfaces tend to increase the emissivity of the surface and therefore the brightness temperature.

The direct emission from calm (flat) seas can be treated precisely with contemporary theory and will be discussed first. Theory describing the emission from rough seas is

not as well developed as for the calm sea case due to the complex nature of the problem. To understand the case of damping by oil films on rough seas it is necessary to consider the more academic problems of the behavior of monomolecular layers on water and of statistics describing the degree of roughness of the ocean surface at various wind speeds.

Calculations of the brightness temperature as a function of oil thickness on flat water show that the brightness temperature oscillates as the thickness increases. The oscillatory nature of the signal can be ascribed to interference effects due to multiple reflections of the waves in the oil layer and will be slowly damped due to attenuation of microwave energy in the oil as greater oil thicknesses are reached. Figures 2-5 show theoretical curves of changes in brightness temperature as a function of oil film thickness for wavelengths of 3.2 and 8.1 mm for horizontal and vertical polarizations. Note that it is possible for thick films (many wavelengths) to give small or even slightly negative temperature anomalies. Theoretical curves may be used to calculate oil film thicknesses on sea water if the dielectric constant of the oil is known and beamfilling conditions are assumed. As an example of what might be encountered in a particular case, consider a film of 30 API gravity crude oil 1.2 mm thick. Neither component of the 3.2-mm wavelength polarizations would show any significant anomaly at an angle of  $45^\circ$ , whereas the 8.1-mm sensors would give anomalies of about  $90^\circ\text{K}$ . The reader is cautioned that these remarks apply only to uniform oil films as opposed to oil films of variable thickness.

In general, the radiometric temperature of a rough ocean is warmer than that of a calm ocean.<sup>2</sup> Thin films of oil on water will damp waves, or decrease the roughness. Therefore, for the case of an oil slick on a rough sea, three major factors must be considered: 1) brightness temperature tends to increase due to the higher emissivity of the oil as discussed above; 2) the horizontal brightness temperature tends to increase significantly in rough seas over the expected temperature for calm seas without the slick; and 3) brightness temperature tends to decrease due to damping of the waves by the oil film. These factors interact in a complex fashion. The predominant effect depends to a large degree, on the sea state and film thickness.

### Laboratory Results

Laboratory studies were conducted to establish the dependence of microwave emission on such parameters as oil thickness, oil type, physical temperature of the oil-water system, observation wavelength, antenna polarization (vertical or horizontal), and antenna viewing angle,  $\theta$ .

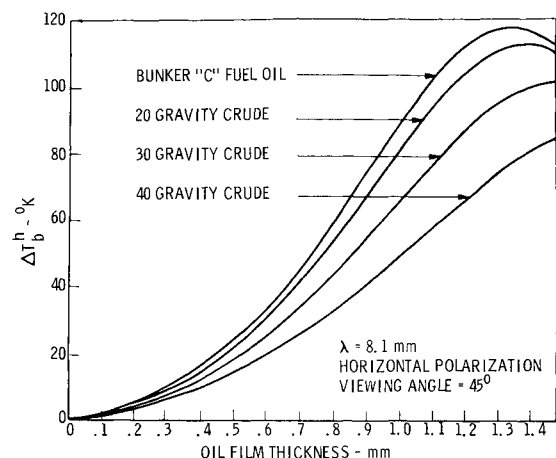


Fig. 3 Horizontal brightness temperature increase,  $\Delta T_b^h$ , vs oil film thickness at 8.1-mm wavelength for smooth water surfaces.

Laboratory data were also used to define the most useful radiometer configuration for at-sea tests.

Radiometric data were taken for gasoline, Bunker "C" fuel oil, 20, 30 and 40 API gravity crude oil using observational wavelengths of 0.81 and 2.2 cm. The dielectric properties of these petroleum products were also measured to facilitate interpretation of the radiometric data. The real and imaginary parts of the dielectric constants were measured and absorptivities were computed as a function of oil film thickness and angle of observation. The imaginary part of the dielectric constant of "fresh" oils was found to be extremely small at 8.1 mm wavelength—less than 0.02 at 23°C. For "fresh" oil, the real part decreases almost linearly with increasing API gravity, and for oil "aged" three days in open air, the real part was found to increase slightly, Fig. 6. The major difference in dielectric properties of "aged" and "fresh" oils appears to occur in the imaginary part. For example, an increase of over two orders of magnitude was observed for Bunker "C" fuel oil. The absorptivity of all oils over ocean water was found to be the same as that of water for oil thicknesses less than 0.1  $\mu\text{m}$ . An increase of less than 0.01 occurred for thicknesses around 0.01 mm.

### Aircraft Measurements

The at-sea tests consisted of airborne measurements of controlled oil spills off the Southern California coast. Dual-polarized 8.1-mm (37 GHz) and 3.2-mm (94 GHz) microwave radiometers were mounted in the fuselage of a twin-engine "Piper Apache" aircraft along with a 35-mm camera, and a K-17 aerial camera. The antennas and 35-mm camera were mounted looking forward of the aircraft at an angle of 45° above nadir. The nadir-oriented K-17 aerial camera (used to map areal distribution of the oil slicks) was mounted forward of the antennas. Both vertical and horizontal outputs of the radiometers were recorded simultaneously on an airborne digital data acquisition system and two dual-channel strip chart recorders.

To satisfy objectives of this effort it was necessary to fly numerous runs across the oil slicks. Normally, measurements began shortly after the spills were formed and continued for about two hours (stay time of aircraft on location). During this period, runs across the slick were made to obtain data when slick sizes and thicknesses were changing rapidly. A surface vessel was used to track and monitor the slick during repeated overflights and until it dissipated. The oil generally spread very rapidly over the water in a nonuniform pattern. The lighter fractions of the oil spread quickly while the heavier fractions re-

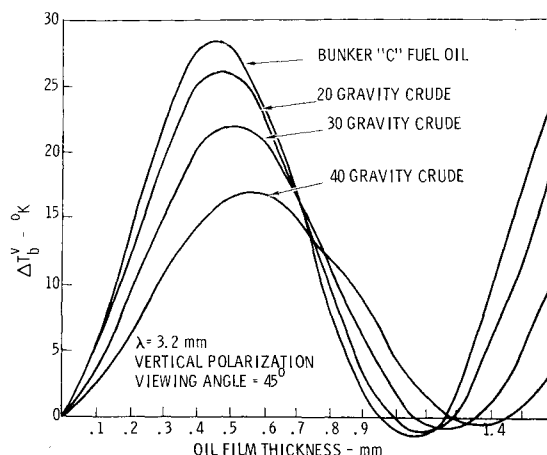


Fig. 4 Vertical brightness temperature increase,  $\Delta T_b^v$ , vs oil film thickness at 3.2-mm wavelength for smooth water surfaces.

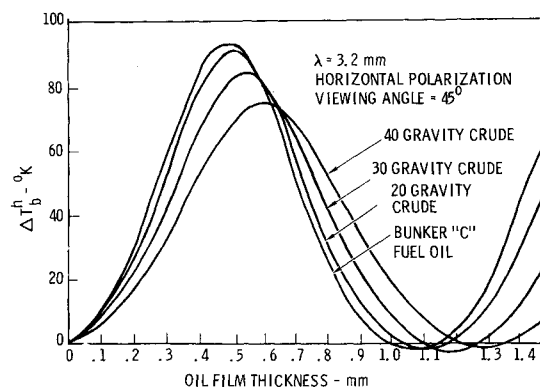


Fig. 5 Horizontal brightness temperature increase,  $\Delta T_b^h$ , vs oil film thickness at 3.2-mm wavelength for smooth water surfaces.

mained localized as patches and streaks. Because of the nonuniformity of the slick, low-level flights were necessary so that specific target areas within a slick could be identified. Most data flights were made at an altitude of 200 ft. At that altitude, the sensor field of view was about 16 × 36 ft. With such a beam size, details of the structure of the slick were obtained.

Aerial photography allowed the size of the slicks to be estimated, and average thickness values calculated. However, due to the complex spreading of the oil, average thicknesses do not correlate with the microwave signatures of the slicks. In the following discussion it must be remembered that, during a single run, the radiometers viewed thick oil, thin films, and water alternately. One notable feature of the slicks, especially those from heavier oil, was that a very heavy streak of oil was common along the leading edge of the slick as it drifted with the wind and current.

The first three missions of the at-sea experiment were performed during periods of low sea state (i.e., sea state ≤ 1). Figure 7 gives representative data of the microwave radiometric responses of the oil spills during periods of low sea state. These data were taken while overflying a 21.6 API gravity crude oil slick spilled during the second mission of the experiment on Oct. 28. As seen from the figure, maximum respective brightness temperature anomalies of 66 and 33°K were measured for the horizontal and vertical polarizations of the 3.2-mm sensor. The

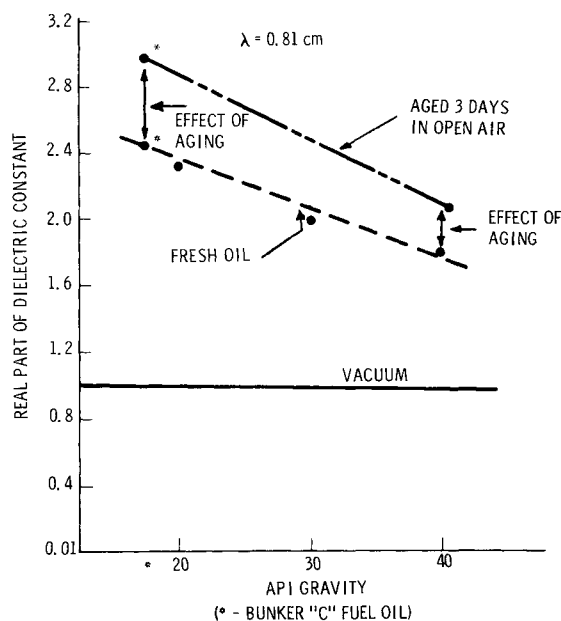


Fig. 6 Dielectric constant of crude oils vs gravity API.

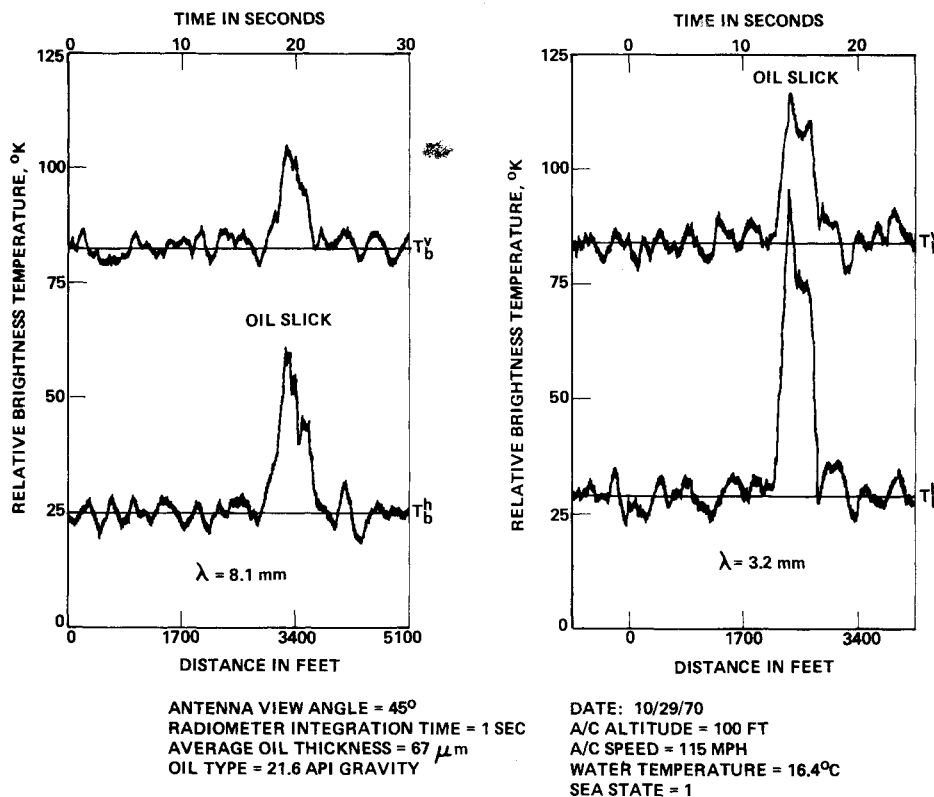


Fig. 7 8.1- and 3.2-mm response to 21.6 API gravity oil.

corresponding 8.1-mm signatures are 36 and 22°K. These anomalies correspond to a theoretical thickness of 0.60 and 0.75 mm for the 8.1-mm radiometer and about 0.36 and 0.5 mm for the 3.2-mm sensor, as calculated from Figs. 2-5. These data were recorded while overflying the long dimension of the slick, and correspond to a calculated average film thickness of 67  $\mu\text{m}$  (based on photography). Note the variations in amplitude of the microwave signals while overflying the slick. This feature is characteristic of oil spills on calm seas and is attributed to variable oil film thickness.

Data were also collected during rough seas. On Nov. 6 two discrete slicks of 660 gallons each of 9.7 and 26.1 API gravity oils were created. The oil slicks were tracked by the surface vessel through Nov. 8. On the second day a surface wind force of 3 (Beaufort scale) prevailed resulting in a 1 to 2-ft chop superimposed on a 6-ft swell. The 26.1 API gravity slick became streaked and dispersed rather

rapidly, as opposed to the 9.7 API gravity slick which remained in a coalesced state through the day.

The 8.1-mm radiometric response to both oil types is shown in Fig. 8. The oil slick signature on a rough sea presents a very complex picture. The vertical component of the brightness temperature is not greatly affected. A slight depression in sea state may be noted for the 26.1 API gravity oil with definite positive peaks of about 6°K for both oil types. The horizontally polarized temperature shows definite sea-state suppression effects by both oil types in addition to showing definite "hot-spots" due to thicker oil patches of 9.7 API gravity fuel. Average decreases in brightness temperature of about 6°K can be measured for both oil types. A positive anomaly of about 8°K exists at the center of the 9.7 API gravity slick, and near the right edge of the first slick there is also an indication of some thicker oil (note the corresponding peaks in the vertical component).

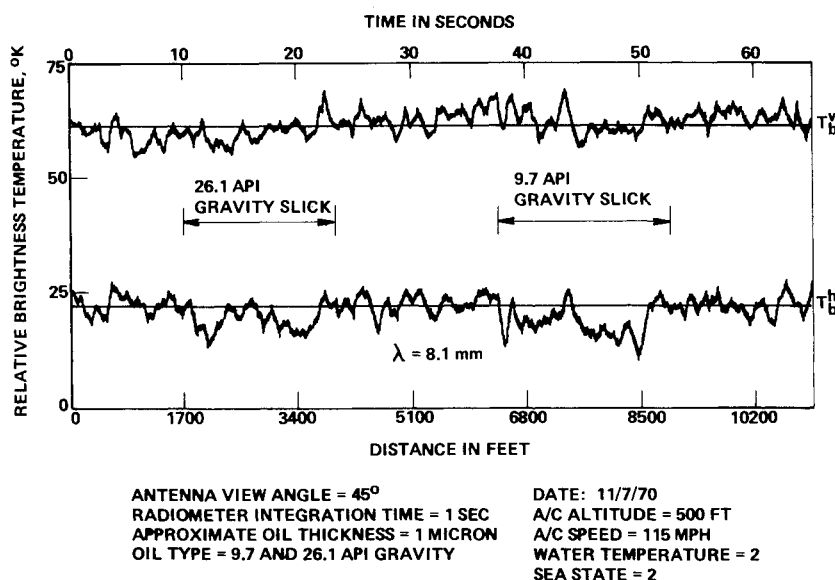


Fig. 8. 8.1-mm response to 9.7 and 26.1 API gravity oil slicks.

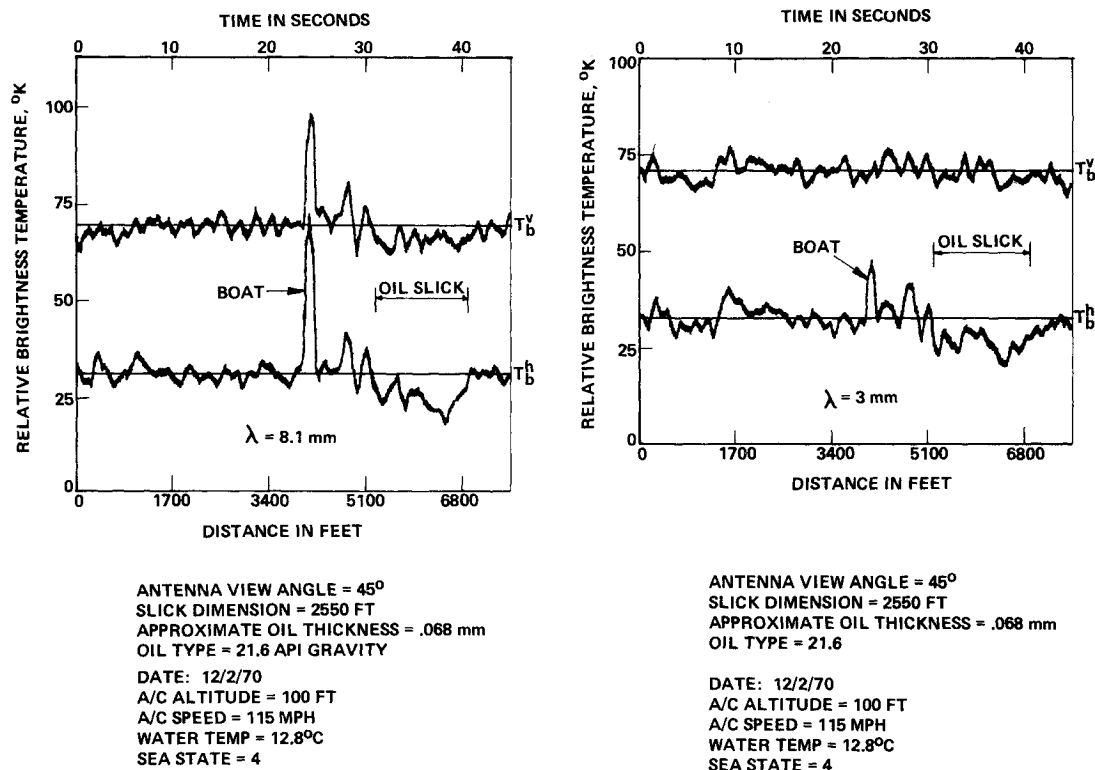


Fig. 9 8.1- and 3.2-mm response to surface vessel and 21.6 API gravity oil slick.

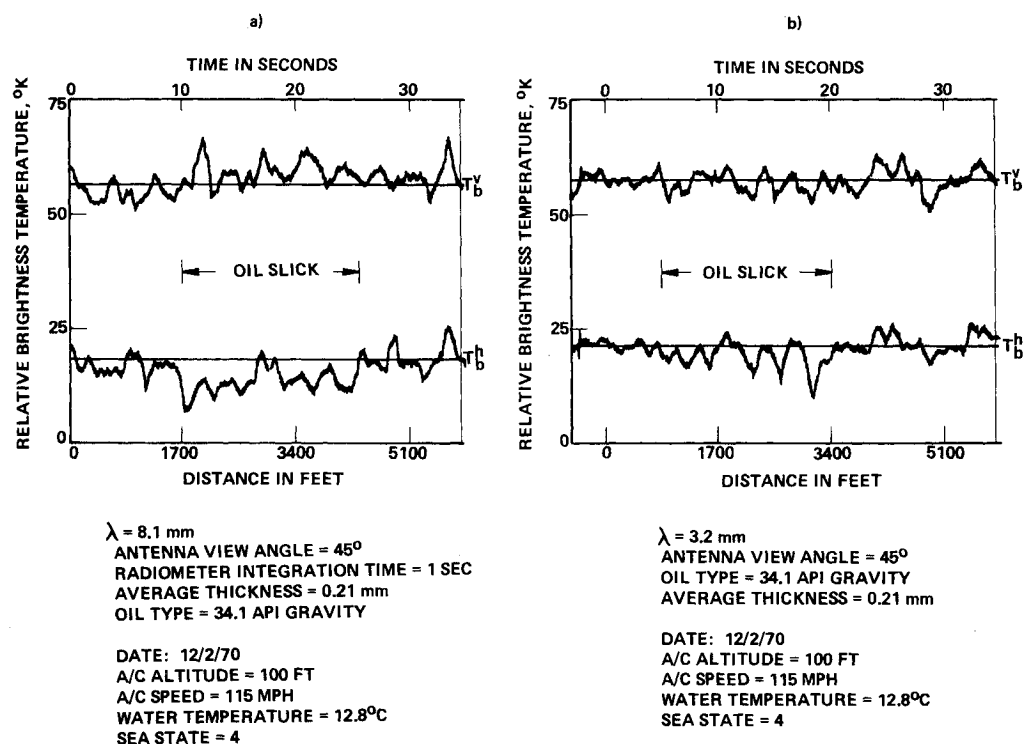
On Dec. 2 the final spills of the experiment occurred. Two discrete slicks of 660 gallons each of No. 2 diesel fuel oil (34.1 API gravity) and 21.6 API gravity crude oil were created. A wind force of 5 (Beaufort scale) prevailed resulting in a 3-7-ft chop superimposed on a 10-ft swell.

Representative 8.1- and 3.2-mm brightness temperature anomalies of the surface vessel and the 21.6 API gravity slick are given in Fig. 9. The vessel gives increases in brightness temperature of 41 and  $29^\circ\text{K}$  for the 8.1-mm horizontal and vertical polarizations, respectively. The low 3.2-mm radiometric anomalies recorded for the sur-

face vessel are probably due to sky reflection effects. The slick, which was immediately adjacent to the vessel, exhibited average 8.1-mm anomalies of  $-7$  and  $-4^\circ\text{K}$  for the horizontal and vertical components, respectively. The recorded horizontal brightness temperature anomaly for the 3.2-mm sensor was  $-7^\circ\text{K}$ . No measureable (above noise) anomaly was noted for the vertical temperature. The calculated average film thickness at this time was  $68\text{ }\mu\text{m}$ .

For the No. 2 diesel oil slick an average horizontal radiometric anomaly of  $-7^\circ\text{K}$  was observed with the 8.1-mm sensor. The vertical component showed only a small posi-

Fig. 10 8.1- and 3.2-mm response to No. 2 diesel oil.



tive anomaly (Fig. 10a). The corresponding 3.2-mm data are shown in Fig. 10b. The slick area at the time of overflight was approximately  $12.5 \times 10^4$  sq ft, indicating an average film thickness of 0.21 mm. The local positive anomalies within the slick area are indicative of thicker segments of oil. Horizontal polarization anomalies are negative, whereas vertical polarization anomalies are absent or slightly positive.

### Conclusions

The phenomena influencing microwave emission by oil slicks interact in a complex fashion in the open-ocean environment giving rise to the following experimental observations. Due to the high emission of the thick oil areas contained in slicks, positive brightness temperature anomalies were noted for all oil films measured on calm seas. For all slicks measured on rough seas, the average horizontal polarization signatures were negative. Thus, the additional emission from the thicker portions of the oil slicks were overshadowed by the decrease in ocean emission associated with the reduction of ocean surface roughness. Positive signatures are superimposed on the negative anomalies suggesting that small areas of thick oil were present in the slick area. As predicted by theory, vertical polarization signatures were generally small, and no correlative patterns were established for oil films on rough seas. It should be noted that negative horizontal temperatures can be uniquely associated with oil slicks, since no other phenomenon is known to cause such a signature in the open-ocean environment.

During the field studies, measured brightness temperature anomalies were generally greater than required for the detection of oil slicks. Lowest amplitude signals were of the order of  $5^\circ\text{K}$ . A  $5^\circ\text{K}$  microwave temperature difference is well within the detection capabilities of passive microwave imaging systems.

The Southern California controlled oil spill experiment, combined with the supporting laboratory and theoretical research concerning the microwave emission characteristics of oil films have yielded the following results. 1) Oil slicks on the ocean surface provide unique and readily measurable signatures. Signatures ranging up to  $70^\circ\text{K}$  were noted while overflying thick portions of oil slicks. All slicks encountered during the controlled oil spills contained thick portions that were detectable. 2) The microwave emission characteristics of oil slicks vary with oil type and film thickness. The mass of oil per unit area is the parameter of most importance. 3) The microwave emission characteristics of oil slicks vary with sea state, and provide measurable signatures over a wide range of sea-state conditions. Oil films with an average thickness of one  $\mu\text{m}$  were readily detected in rough seas with 3.2-

and 8.1-mm sensors. 4) Both theory and measurements demonstrate that horizontally polarized sensors are more responsive to oil films than vertically polarized sensors. 5) The microwave brightness temperature signatures of oil slicks increase with sensor frequency (vary inversely with sensor wavelength). However, atmospheric attenuation also increases with frequency. The available atmospheric and oil film signature data indicate that a frequency (wavelength) of about 37 GHz (8.1 mm) is optimal.

These results indicate that imaging microwave radiometers can be employed to detect and map oil slicks. The writers recommend a horizontally polarized, 8.1-mm (37 GHz) imager with a constant viewing angle of  $45^\circ$  and real-time video display for this purpose. This system will provide adverse weather, as well as day and night detection capabilities.

Additional observations concerning the behavior of oil films on the ocean surface may be of interest and are noted below. 1) The oil slicks formed on the ocean surface all exhibited significant point-to-point variations in thickness. Even the slicks formed under near-ideal conditions spread in a nonuniform fashion. For example, point source spills of low viscosity oil on a calm ocean surface exhibited thickness variations exceeding the average calculated thickness (volume of spill divided by total area of slick) by two or more orders of magnitude. 2) Oil slicks modify sea state by reducing surface roughness, particularly the higher frequency components such as wavelets, small scale waves, breaking waves, etc. Many investigators have considered the physics of sea-state suppression due to oil films, and have developed strong evidence, both theoretical and experimental, that sea-state suppression by an oil film is essentially independent of film thickness. That is, damping due to monomolecular and comparatively thick oil films of interest in oil pollution surveillance give rise to very similar sea-state reductions. Experimental data collected during the Southern California controlled oil spills are consistent with the hypothesis. 3) If this hypothesis is correct, all natural oil films (fish oil, etc.) small legally acceptable man-made spills, etc., will cause similar sea-state suppression, and sensors that rely exclusively on detection of this effect must contend with a potentially large false alarm rate. This relationship should be examined more closely.

### References

- <sup>1</sup>Meeks, D. et al, "Microwave Radiometric Detection of Oil Slicks," Rept. 1335-2, March 1971 (Contract DOT-CG-93, 228A), Aerojet-General Corp., El Monte, Calif.
- <sup>2</sup>Stogryn, A., "The Apparent Temperature of the Sea at Microwave Frequencies," *IEEE Transactions on Antennas and Propagation*, AP-15, No. 2, March 1967, pp. 278-286.